Site characterization of rare-earth-doped LiNbO$_3$ using total site selective spectroscopy

D. M. Gill
University of Wisconsin-Madison, Materials Science Program, Madison, Wisconsin 53706

J. C. Wright
University of Wisconsin-Madison, Chemistry Department, Madison, Wisconsin 53706

L. McCaughan
University of Wisconsin-Madison, Electrical and Computer Engineering, Madison, Wisconsin 53706

A technique, total site selective spectroscopy, is presented to optically identify spectroscopic sites in Er:LiNbO$_3$. Six sites are seen; four major nonclustered sites and two minor cluster sites. When pumping the $^4F_{9/2}$ manifold at low temperatures ($\sim$12 K), only cluster sites are found to upconvert using a nonradiative energy transfer mechanism. The polarization of Er^{3+} absorption cross sections are shown to be site dependent while the manifold lines from different sites are highly degenerate. These characteristics likely contribute to the observed simultaneous lasing at two wavelengths of devices based in this medium.

LiNbO$_3$ is an active host for guided wave optics in which the most advanced integrated optic systems have been produced.[1] Guided wave (cw) lasers and travelling wave amplifiers have been reported in Er^{3+}- and Nd^{3+}-doped LiNbO$_3$.[2–4] Efforts to optimize rare-earth-doped LiNbO$_3$ devices have mainly focused on waveguide and cavity fabrication.[2–6] Materials engineering of the gain media itself has not been addressed. This is, in part, because characterization using only standard site-selective spectroscopy yields incomplete results.[7,8] An understanding of site character and distribution will help facilitate materials engineering of these gain media and lend insight into new applications. For example, Er^{3+} is a rare-earth ion whose long lived $^4I_{13/2}\rightarrow ^4I_{15/2}$ transition produces $\sim$1.5 μm light, one of the principle carrier wavelengths in telecommunications. Er:LiNbO$_3$ lasers display upconversion,[9] the source of which has not been established. Upconversion can arise from two processes: excited state absorption and/or nonradiative energy transfer. Excited state absorption, in any medium, is a fundamental consequence of a given pump/signal choice, and is difficult to change. Conversely, nonradiative energy transfer arises from a distinct subset of the total Er^{3+} population, namely cluster sites, and can be enhanced or suppressed by changing the relative concentration of these sites.[10,11] As another example, Er:LiNbO$_3$ lasers can also be made to simultaneously lase at 1563 and 1576 nm in the σ and π polarizations, respectively, if pumped at 1479 nm in the π polarization. This effect is also not yet understood.[4] In this letter, we identify and characterize, for the first time, the site distribution of Er^{3+} in LiNbO$_3$.

Rare-earth dopant ions have optically active transitions which are shielded by outer electrons. Single ion transition lines are sharp and express themselves as groups of Stark split manifold levels (Fig. 1). Ions whose sites have different symmetries tend to have differences in their crystal field splittings. Therefore, site subpopulations can be "finger printed" by determining the transition energies specific to each rare-earth site. Since a given site's absorption line is broad in LiNbO$_3$ compared to that of many other crystalline hosts (Fig. 1), it is important to acquire more detailed spec-

troscopic information through total site selective spectroscopy. Total site-selective spectroscopy involves three-dimensional spectra of low temperature (12 K), fluorescence, and fluorescence excitation data. The technique was previously used by Weber in the analysis of multicomponent suspensions in solution.[12]. The monitored fluorescence wavelength is incremented after each excitation scan in steps much smaller than the breadth of the electronic states considered. The excitation and fluorescence wavelengths are plotted along the x and y axes while the fluorescence intensity is plotted as constant intensity contours. This format displays all the excitation and fluorescence information about a system from which correlations between features can be determined. Figure 1 shows important features of this format in a schematic way for the $^4F_{9/2}\leftrightarrow ^4I_{15/2}$ transition. There are five states labeled a–e in the $^4F_{9/2}$ manifold and eight states in the $^4I_{15/2}$ manifold. Radiative and nonradiative tran-
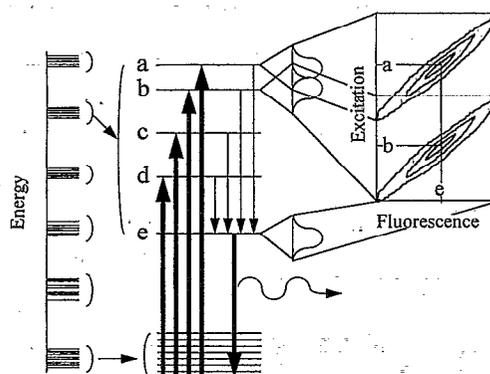

FIG. 1. Schematic diagram of important features of the total site-selective contour plot in Fig. 2. Radiative and nonradiative transitions are indicated by broad and narrow arrows, respectively. Only transitions pertinent to Fig. 2 are shown. The middle portion of the figure represents the $^4F_{9/2}$ crystal field lines (labeled a–e) for one site. Inhomongeneous broadening in LiNbO$_3$ is indicated for lines a, b, and e. The far right of the figure shows a total site selective spectrum with the excitation energies of transitions to the a and b lines plotted on the y axis and the fluorescence wavelength of transitions from line e plotted on the x axis. Fluorescence intensity is plotted as constant intensity contours.
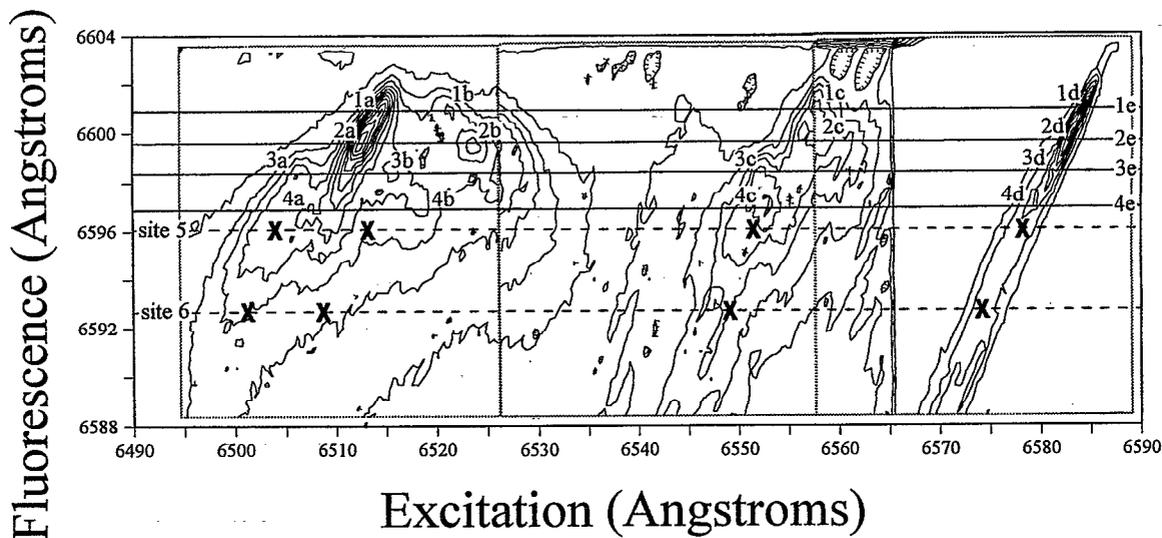
FIG. 2. Total site-selective contour plot of data from the $^4F_{9/2} \leftrightarrow ^4I_{15/2}$ transition in a poled 1.0 mol % Er:LiNbO$_3$ crystal. The $^4F_{9/2}$ manifold was pumped with a pulsed (~5 ns) x-propagating beam linearly polarized at 45° to the y and z crystallographic axis. Sites are labeled 1–6, $^4F_{9/2}$ manifold levels are labeled a–e. The X's represent $^4F_{9/2}$ manifold line positions for the two cluster sites as determined from Fig. 4. (Excitation linewidth width ~0.4 Å, fluorescence resolution ~0.5 Å.)

sitions are shown by the broad and narrow arrows, respectively. The middle portion of the figure represents the inhomogeneous broadening of the a, b, and e states for a given site. The far right of the figure shows a total fluorescence spectrum with the excitation energies of the a and b transitions plotted on the y axis while the fluorescence wavelength of transitions from state e are shown on the x axis. The intensity contours show that there is correlation between the excitation and fluorescence transitions for different points in the inhomogeneous envelope. If there were no correlation, the elliptical contours would not be tilted. If there were several sites, the centers of the elliptical contours would be displaced from each other.

A congruent, poled Er:LiNbO$_3$ crystal was obtained from the Tianjin University, P. R. China, with an Er concentration of 0.5 mol % Er$_2$O$_3$ (1.0 mol % Er:LiNbO$_3$). Samples were mounted in a closed cycle cryostat and cooled to ~12 K. The crystal was excited with a pulsed (~5 ns) tunable dye laser (FWHM ~0.4 A). Fluorescence was monitored with a 1 m monochromator and measured with a dry ice cooled photomultiplier tube and a gated integrator.

Figure 2 is a total site-selective spectrum for the $^4I_{15/2} \leftrightarrow ^4F_{9/2}$ transition whose excitation was linearly polarized at 45° between the y and z crystallographic axes. Figure 3 shows the polarization characteristics of one feature. The elliptical contours of the different sites can be recognized in these spectra and their centers are identified with labels where the number indicates the site and the letter indicates the particular transition (using Fig. 1 notation). Horizontal lines identify the fluorescence maximum of each site. A complementary total site selective spectrum of the $^4I_{15/2} \rightarrow ^4F_{9/2}$ excitation transition and $^4S_{3/2} \rightarrow ^4I_{15/2}$ upconverted fluorescence transition is shown in Fig. 4. Since Figs. 2 and 4 have the same x axes, the correlation between the spectra can be determined. The $^4F_{9/2}$ crystal field levels, identified in Fig. 4 with X's, are marked at the same wave-
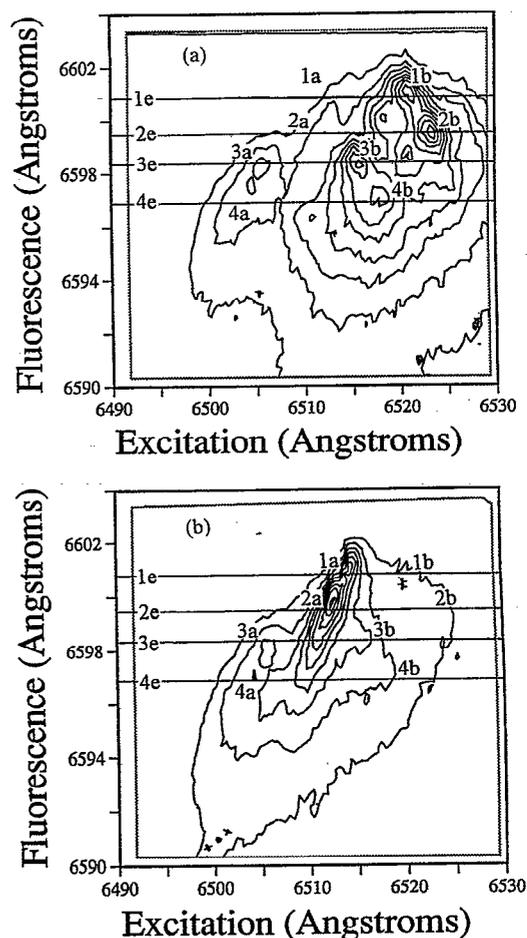

FIG. 3. Total site-selective contour plot of data from the $^4F_{9/2} \leftrightarrow ^4I_{15/2}$ transition. Sites are labeled 1–4, $^4F_{9/2}$ manifold levels are labeled a, b, and e. (Excitation line width ~0.4 Å, fluorescence resolution ~0.5 Å): (a) with the excitation beam π polarized (x propagating, linearly polarized parallel to the z axis); (b) with the excitation beam σ polarized (x propagating, linearly polarized perpendicular to the z axis).

Gill, Wright, and McCaughan
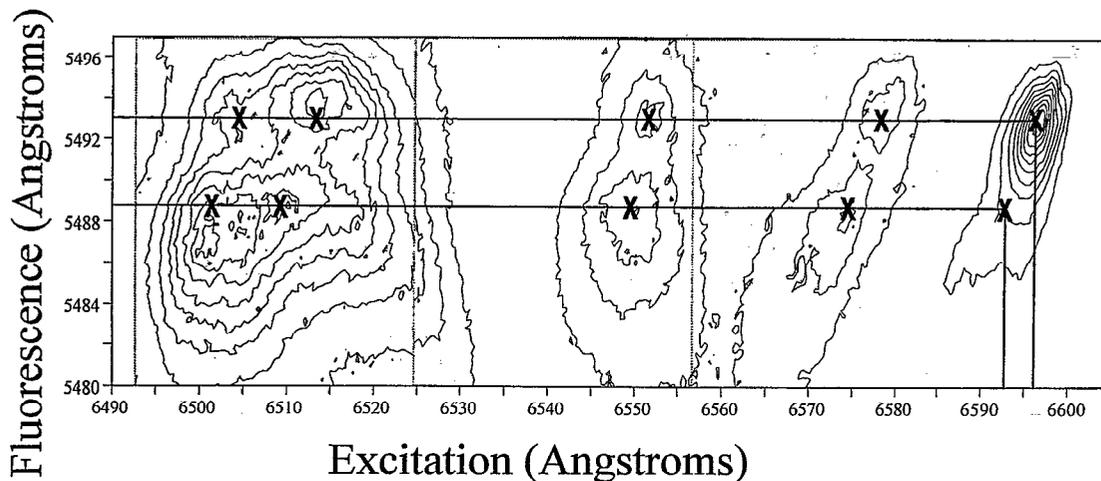
FIG. 4. Total site-selective contour plot of upconverted fluorescence $^4S_{3/2} \rightarrow ^4I_{15/2}$ transition) while pumping to the $^4F_{9/2}$ manifold. The excitation beam was x propagating and unpolarized. Sites are identified with solid lines and $^4F_{9/2}$ manifold crystal field levels (lines a–e) are labeled with X's. The vertical lines indicate the wavelengths at which the upconverting sites should produce nonupconverted fluorescence. (Excitation line width ~0.4 Å, fluorescence resolution ~3 Å).

lengths in Fig. 2 and identified as sites 5 and 6. No peaks are seen at those positions in Fig. 2 because the concentrations of the sites are too low.

Sites 1–4 are divided into 2 groups, sites 1 and 2 and sites 3 and 4, on the basis of the similarities in their spectra, absorption cross section polarizations, and fluorescence lifetimes.[13] Sites 1 and 2 have strongly polarized transitions (see Fig. 3) while sites 3 and 4 have weak polarization dependencies. Assuming the Er ions exclusively substitute at Li and Nb lattice locations, as has been shown for Eu^{3+} in $Eu:LiNbO_3$,[14] we suggest that one pair of similar sites represents Er ions in two different Li sites and the other pair represents Er ions in two Nb sites. The difference in the polarization of the absorption cross sections between the two pairs of sites probably contributes to the simultaneous lasing of the 1563 and 1576 nm lines in $Er:LiNbO_3$ lasers. [4]

Sites 5 and 6 are distinctly different from the others because they exhibit strong upconversion spectra as shown in Fig. 4. Up conversion is observed from the $^4G_{11/2}$ (~388 nm), $^2H_{9/2}$ (~412 nm), and $^4S_{3/2}$ (~540 nm) manifolds when the $^4F_{9/2}$ manifold is excited. We assign the upconverting mechanism to energy transfer between two excited Er ions that are clustered. The alternate mechanism, a sequential two-step absorption (excited state absorption), is unlikely for three reasons: upconversion is not observed for the major sites despite the similarity of their electronic states to the minor upconverting sites; there are no absorbing levels at the wavelengths required for sequential absorption of the 5 ns excitation pulse; and finally, the quantitative fittings we have made of fluorescence transient kinetics is consistent with energy transfer but not with sequential absorption.[13] This result is specific to pumping the $^4F_{9/2}$ manifold. Upconversion reported when pumping to $^4I_{13/2}$ (~1480 nm) manifold is probably from a combination of excited state absorption and energy transfer since absorbing levels are available for excited state absorption.

In conclusion, a generally applicable spectroscopic technique, total site selective spectroscopy, is used to optically characterize rare-earth-doped $LiNbO_3$. We have identified six sites in $Er:LiNbO_3$, two of which are cluster sites. Nonradiative energy transfer in cluster sites is the dominant source of upconversion when pumping the $^4F_{9/2}$ manifold (at ~12 K). Therefore, insight can be gained into the degree of Er clustering by comparing upconverted spectra to nonupconverted spectra while pumping this manifold. We observe that the polarization of absorption cross sections in $Er:LiNbO_3$ are site dependent while the crystal field lines from different sites are relatively degenerate. This result is consistent with the observed simultaneous lasing of two wavelengths in $Er:LiNbO_3$ devices. We suggest that total site selective spectroscopy may be extended to the study of energy transfer in co-doped systems (e.g., Yb:Er-doped $LiNbO_3$ and glass fiber).

[1] R. C. Alferness, Guided Wave Optoelectronics, edited by T. Tamir (Springer, New York, 1988), p. 145.

[2] A. Cordova-Plaza, M. J. Digonnet, and H. J. Shaw, IEEE J. Quantum Electron. QE-23, 262 (1987).

[3] E. Lallier, J. P. Pocholle, M. Papuchon, M. P. De Micheli, M. J. Li, Quig He, D. B. Ostrowsky, C. Grezes-Besset, and E. Pelletier, Opt. Lett. 15, 682 (1990).

[4] P. Becker, R. Brinkmann, M. Dinand, W. Sohler, and H. Suche, Appl. Phys. Lett. 61, 1257 (1992).

[5] D. M. Gill, A. Judy, L. McCaughan, and J. C. Wright, Appl. Phys. Lett. 60, 1067 (1992).

[6] C. H. Huang, D. M. Gill, and L. McCaughan, J. Lightwave Technol. (1994) (to be published).

[7] J. E. Munoz Santiuste, B. Macalik, and J. Garcia-Sole, Phys. Rev. B 47, 88 (1993).

[8] J. O. Tocho, E. Camarillo, F. Cusso, F. Jaque, and J. Garcia-Sole, Solid State Commun. 80, 575 (1991).

[9] R. Brinkmann, W. Sohler, and H. Suche, Electron. Lett. 27, 415 (1991).

[10] K. M. Cirillo-Penn and J. C. Wright, Phys. Rev. B 41, 10799 (1990).

[11] D. S. Moore and J. C. Wright, J. Chem. Phys. 74, 1626 (1981).

[12] G. Weber, Nature 190, 27 (1961).

[13] D. M. Gill, J. C. Wright, and L. McCaughan (unpublished).

[14] L. Rebouta, J. C. Soares, M. F. da Silva, J. A. Sanz-Garcia, E. Dieguez, and F. Agullo-Lopez, Appl. Phys. Lett. 55, 120 (1989).

Appl. Phys. Lett., Vol. 64, No. 19, 9 May 1994

Gill, Wright, and McCaughan   2485